

TreeSegNet: Automatically Constructed Tree CNNs for Subdecimeter Aerial Image Segmentation

Kai Yue, Lei Yang, Ruirui Li* , Wei Hu, Fan Zhang, Wei Li

Beijing University of Chemical Technology, Beijing, China

College of Information Science & Technology

Abstract

For the task of subdecimeter aerial imagery segmentation, the fine-grained semantic segmentation results are usually difficult to obtain because of complex remote sensing contents and optical conditions. In addition, remote sensing imagery has inherent limitations of imbalanced class distribution. Recently, convolutional neural networks (CNNs) have shown outstanding performance on this task. In this paper, we propose the TreeSegNet to solve the class imbalance problem and further improve the accuracy in the metrics' point of view. Based on the infrastructure of DeepUNet, a Tree-CNN model in which each node represents a ResNeXt unit is constructed automatically according to confusion matrix and minimum graph cut algorithm. By transporting feature maps by concatenating connections, the Tree-CNN block fuses the multiscale features and learning the best weights for the model. In the experiments on ISPRS 2D semantic labeling Potsdam dataset, the results gotten by TreeSegNet are better than the opened state-of-the-art methods. The F1 measure scores of classes are improved especially for those classes

* Corresponding author. Tel.: +86 18911938368. E-mail address: ilydouble@gmail.com

that are easily confused. Completely and detailed comparison and analysis are performed to show that the improvement is brought by the construction and the embedding of the Tree-CNN module.

keywords: aerial imagery, semantic segmentation, tree CNNs, automatic constructing, ISPRS, ResNeXt,

1. Introduction

Semantic segmentation is the task of assigning a semantic label (land-cover or land-use class) to every pixel of an image. Recently, the highly developed remote sensing techniques can provide very-high-resolution (VHR) aerial images with a ground sampling distance (GSD) of 5-10cm in the spatial or spectral domain. As a result, small objects such as cars and buildings are distinguishable and are able to be segmented. When processing ultrahigh resolution data, most of the previous state-of-the-art methods rely on supervised classifiers trained on specifically hand-crafted feature sets, describing locally the image content. The extracted high-dimensional representation is assumed to contain enough information to classify a pixel. However, these features depend on a specific feature extraction method whose parameters and performance on the specific data are priori unknown.

The deep convolutional neural networks (DCNNs) have become extremely successful in many high-level computer vision tasks, ranging from image classification [1] to object detection, visual recognition, and semantic segmentation. DCNNs deal with the trainable task in an end-to-end fashion, which usually means learning jointly a serious feature extraction from raw input data to a final, task-specific output. DCNNs have also applied to remote sensing field. Fully convolutional network (FCN) [2] is a classic DCNN which is designed for semantic segmentation. Sherrah et al. [3] applied the FCNs to remote

sensing imagery and published their results on the ISPRS Potsdam benchmark. The extension of FCN, including DeconvNet [4], SegNet [5] and U-Net [6] are then used in aerial imagery labeling [7-9] for higher accuracy.

Even for the existing well-performed DCNN network structures, semantic labeling for aerial imagery is still difficult. The VHR images are typically containing tens to hundreds of megapixels and a potentially-unlimited continuous scene. For such images, the semantic labeling DCNNs are required of better comprehension of image context and producing higher accuracy models. Moreover, as often observed, aerial imagery is characterized by complex data properties in the form of heterogeneity and class imbalance.

In this paper, we proposed the TreeSegNet architecture which contains an automatically constructed Tree-CNN module. The Tree-CNN module combined with the new short connections are designed for class imbalance problem in multi-class labeling. The TreeSegNet is based on the DeepUNet [10] and provides a better accuracy than that of the state-of-the-art methods on the ISPRS Potsdam dataset. In summary, we made but not limited to the following contributions to the community:

- 1) The TreeSegNet provides a better result on the ISPRS Potsdam dataset than other state-of-the-art methods.
- 2) An automatically constructed TreeSegNet is proposed to face the complex data properties and to solve the class imbalance problem. As far as we know, it is the first automatically adapted CNN for multi-class labeling tasks.
- 3) A novel modified DeepUNet is introduced to semantic labeling the VHR remote sensing images which adopted the ResNeXt concept.
- 4) A group of thoroughly complete experiments are performed on the ISPRS Potsdam dataset, making comparisons among U-Net, DeepUNet, and TreeSegNet.

The remainder of the paper is organized as follows. In Section 2, we will introduce the research topics related to the subjects including remote sensing semantic labeling, deep learning and imbalance data classification. The method proposed in this paper will be described in Section 3. Section 4 shows training details that include data preprocessing, training parameters, and post-processing image stitching. And Section 5 discusses the experimental situation and analyses the results. The last section shows the conclusions of this paper.

2. Related works

2.1 Semantic segmentation for remote sensing imagery

The nature of semantic segmentation on remote sensing images is to classify houses, vehicles, roads, vegetation, oceanic ice and etc. in pixel-wise precision. The remote sensing images come from aerial imagery or spectroscopy sensors. Early works are primarily based on graph theory (Shi J, Malik J, 2000 [11]; Boykov Y, Jolly M P, 2001 [12]; Grady L, 2006 [13]; Grady L, Eric L, Schwartz, 2006 [14]) using the unsupervised learning [15]. In 2009, Ye et al. [16] put forward a new segmentation method on remote sensing imagery by combining the minimum spanning tree algorithm with Mumford Shah theory. Cui, Zhang et al. [17] proposed a multi-scale and multi-level segmentation method based on minimum spanning tree in 2011 which performed well in high resolution remote sensing image segmentation. For supervised learning, most segmentation methods selected features by hand [18-22]. These features are generally complex and can only express low or mid-level descriptions.

With the development of remote sensing technologies, a large number of VHR remote sensing images can be easily obtained. These images have a wealth of contextual information, making most of the traditional segmentation methods unsuitable. CNNs

learn hierarchical semantic features of images through the end-to-end training and can be applied to remote sensing image segmentation. The Fully Convolutional Networks (FCNs) first came from Long et al. at Berkeley is a milestone. It replaces all fully connected layers with convolutional neurons to allow arbitrary image size segmentation. Dilated convolution [23] provides a larger receptive field under the same computational conditions. It could be used as pooling operation to do dimensionality reduction. Lots of works are proposed to improve the dilated convolution including atrous spatial pyramid pooling [24], fully connected CRF [25] and etc. Inspired by the encoder-decoder architecture, SegNet [26], DeconvNet[4], RefineNet [27] and U-Net[28] were proposed to handle pixel-level segmentation. Recently, the gated segmentation network (GSN) [29] added gated thresholds to the CNN. It did experiments on the ISPRS 2D semantic labeling benchmark and achieved a competitive result of overall accuracy on the Potsdam dataset.

2.2 Multi-class imbalance problem

For the multi-class segmentation problem, the following two questions are of crucial importance: first, the multi-class dataset has an imbalanced distribution; secondly, there exist easily confused classes in the nearby areas. For different categories, the quantity and the distribution of the training data vary, leading to different segmentation capabilities. The visual similarity of easily confused classes often makes the situation worse and causes the errors and inconsistency of annotations.

Most approaches proposed in the literature fall into one of these three groups: a) to design better learning techniques, for instance, ensemble learning, b) to apply some kinds of transformation over the training data, and c) to modify or adjust the predictions given by the classifier, for instance, classifier calibration techniques [30, 31]. In group b), a direct way to deal with imbalanced datasets [32] is to handle the class representations of

an original dataset by sampling techniques [33] or by feature selection [34, 35]. These techniques change the raw distribution of data, thus sacrificing comentropy that sample data carries. Ensemble learning [36, 37] is a machine learning paradigm where multiple learners are trained to solve the same problem. There is a theoretical research conducted in 1989, where Schapire [38] proved that weak learners can be boosted to strong learners.

Since the emergence of CNN, deep ensemble learning becomes a research hotspot where training data are insufficient. Several works focus on improving the learning strategy by designing a new neural network architecture that combines multiple learning tasks [39, 40]. The AdaBoost-CNN [41], referred to as ACNN, can solve the problem of class recognition rate imbalanced caused by similar categories or training samples quantity deviation. Some efforts also have been made to reduce the training and testing cost for ensembles. Hinton et.al and Balan et.al. [42] distill the knowledge of an ensemble into a single model. Though the cost problem is not what the paper mainly concerned, our approach adopts the similar concept that learning a structure and assembling it into an end-to-end convolutional neural network.

3. Proposed method

For multi-class labeling tasks, it is difficult to learn semantic representations for pixels because of the imbalanced distribution of classes in remote sensing images. Based on the observation that classes may share some features while possessing their own properties, we try to address the imbalance multi-class labeling problem by hierarchically organize the neural modules into a collection of sub-groups and provide the easily confused classes more convolutional computations. To do this in an end-to-end fashion, we propose a novel CNNs architecture called TreeSegNet for semantic segmentation on remote sensing images. The main framework is illustrated in Fig 1.

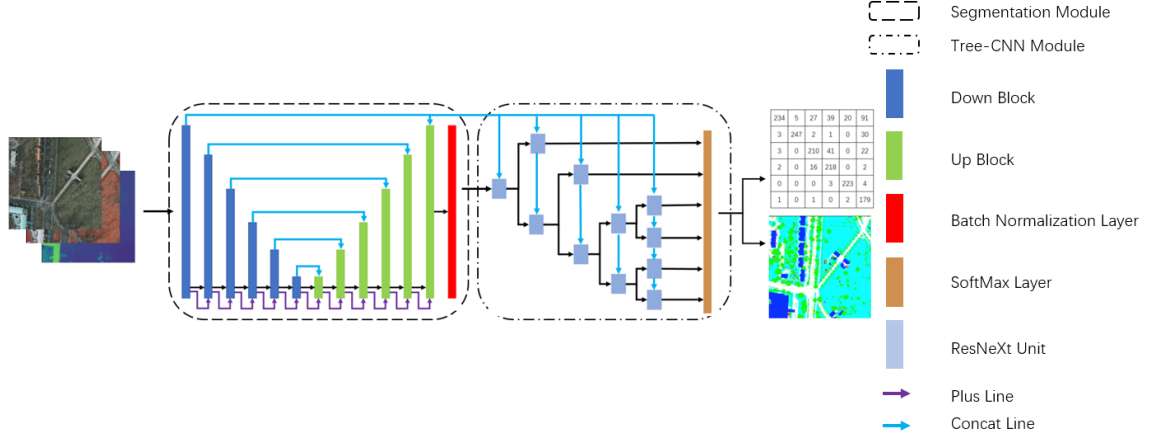


Fig 1. the TreeSegNet framework

The TreeSegNet architecture is mainly composed of three parts: the segmentation module, the Tree-CNN module, and the concatenating connections. We choose the DeepUNet structure for the segmentation module. A batch normalization connects the DeepUNet module and the Tree-CNN module. The Tree-CNN module is built by an automatic construction method according to the confusion degree between the pair of classes. For the first time, the method has to train an initial model and compute the confusion matrix from the first-time running result. In the following passes, the TreeSegNet is updated by adding a new Tree-CNN module. The semantic segmentation model is finely retrained by the new network structure to further optimize the accuracy. The processing will be iterated a few of passes until the confusion matrix gets convergent. This section begins with the main framework of the TreeSegNet, which introduces the basic idea and the architecture first. Then we describe segmentation module and the Tree-CNN module in detail with which together greatly enhance the performance of the neural network when dealing with segmentation tasks with imbalance and easily confused classes.

3.1 Segmentation module

As shown in Fig 1, we use the DeepUNet as the infrastructure network for pixel-wise

semantic segmentation. The DeepUNet is based on the VGG16 [43]. It has two processing paths as the U-Net. They are the contracting path and the expanding path. In the contracting path, the DownBlock is used as the basic feature extraction module. It contains two convolutional layers and one pooling layer. Symmetrically, in the expanding path, the UpBlock is used as the up-sampling block. Features are passed from the DownBlock to the UpBlock of the same level and then concatenated to perform convolution and up-sampling. Both the DownBlocks and the UpBlocks use the residual operations and skip connections which allows the DeepUNet superior to other similar CNN architectures such as U-Net and DeconvNet.

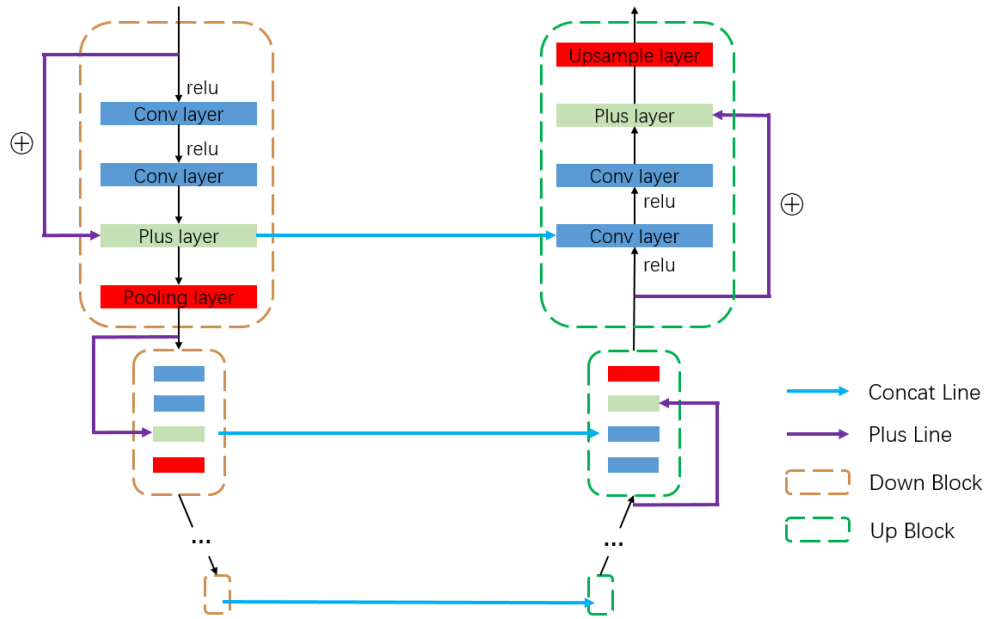


Fig 2. DeepUNet network structure

Fig 2 shows the segmentation network of DeepUNet. There are two kinds of connections. The blue lines are concatenating connections which transfer features from left side to the right side. The purple lines are skip connections to perform residual operations. The structure surrounded by the brown dotted rectangle is the DownBlock, and that surrounded by the green dotted rectangle is the UpBlock. In the DownBlock, two

successive 3x3 convolutional layers are used instead of one 5x5 layer. This allows the block obtain the same receptive field with fewer hyperparameters. A Plus layer is added after the convolution operations and leaves the intermediate result into the pooling layer. The structure of the UpBlock is symmetric. Differently, the pooling layer in the DownBlock is replaced by the up-sampling layer in the UpBlock.

3.2 Tree-CNN module

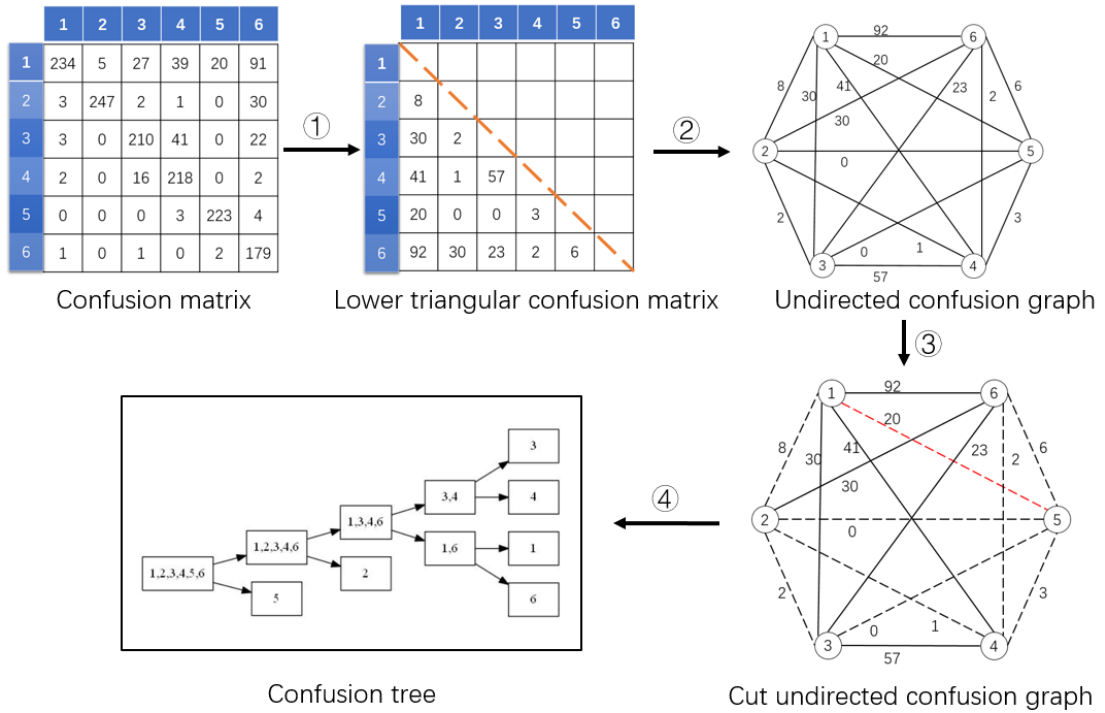


Fig 3. The construction processing of Tree-CNN module.

As Fig 3 shows, the construction of Tree-CNN module is started by calculating the confusion matrix according to the first-time running result. The confusion matrix, also known as an error matrix, is a specific table layout that allows visualization of the performance of an algorithm. Each row of the matrix represents the instances in a predicted class while each column represents the instances in an actual class (or vice versa). With the confusion matrix, to construct the tree-like neural layers, there are following four steps:

- ① Calculating lower triangular matrix;
- ② Building undirected graph;
- ③ Iterated minimum graph cutting;
- ⑤ Constructing the tree structure;

In the confusion matrix, we use a_{ij} to represent the element of the i -th row, j -th column; b_{ij} to represents the value in the lower triangular confusion matrix. According to the following equation, a lower triangular matrix is obtained by adding the values of the symmetric positions. b_{ij} represents the confusion degree between class i and class j .

$$b_{ij} = \begin{cases} a_{ij} + a_{ji}, & i > j \\ 0, & \text{otherwise} \end{cases}$$

The lower triangular matrix can be seen as an adjacency matrix which is associated with an undirected graph. In the graph, nodes represent the indices of classes and the values on connections represent the weight of confusion. Numbers 1-6 represent imp_surf, building, low_veg, tree, car, and clutter respectively.

3.2.1 Iterated minimum graph cutting

The undirected graph is then transformed into a binary tree structure by the minimum graph cut algorithm. The pseudo-code of the algorithm is illustrated in the Algorithm 1. It nestedly cuts the edge with the lowest weight in the current graph and splits the graph into two subgraphs until there is no edge to cut.

Algorithm 1 The algorithm for the proposed Graphcut operation

Input: The lower triangular confusion matrix B

The undirected confusion graph G

Output: The binary tree-like structure T

```
1: while  $G$  still has edges do
2:   choose the edge of the lowest weight  $e$ 
3:    $G \leftarrow G - e$ 
4:   if  $G$  is still a complete graph then
5:     continue
6:   elif  $G$  are cut into two subgraphs  $G1$  &  $G2$  then
7:     Graphcut( $G1$ )
8:     Graphcut( $G2$ )
9: end while
```

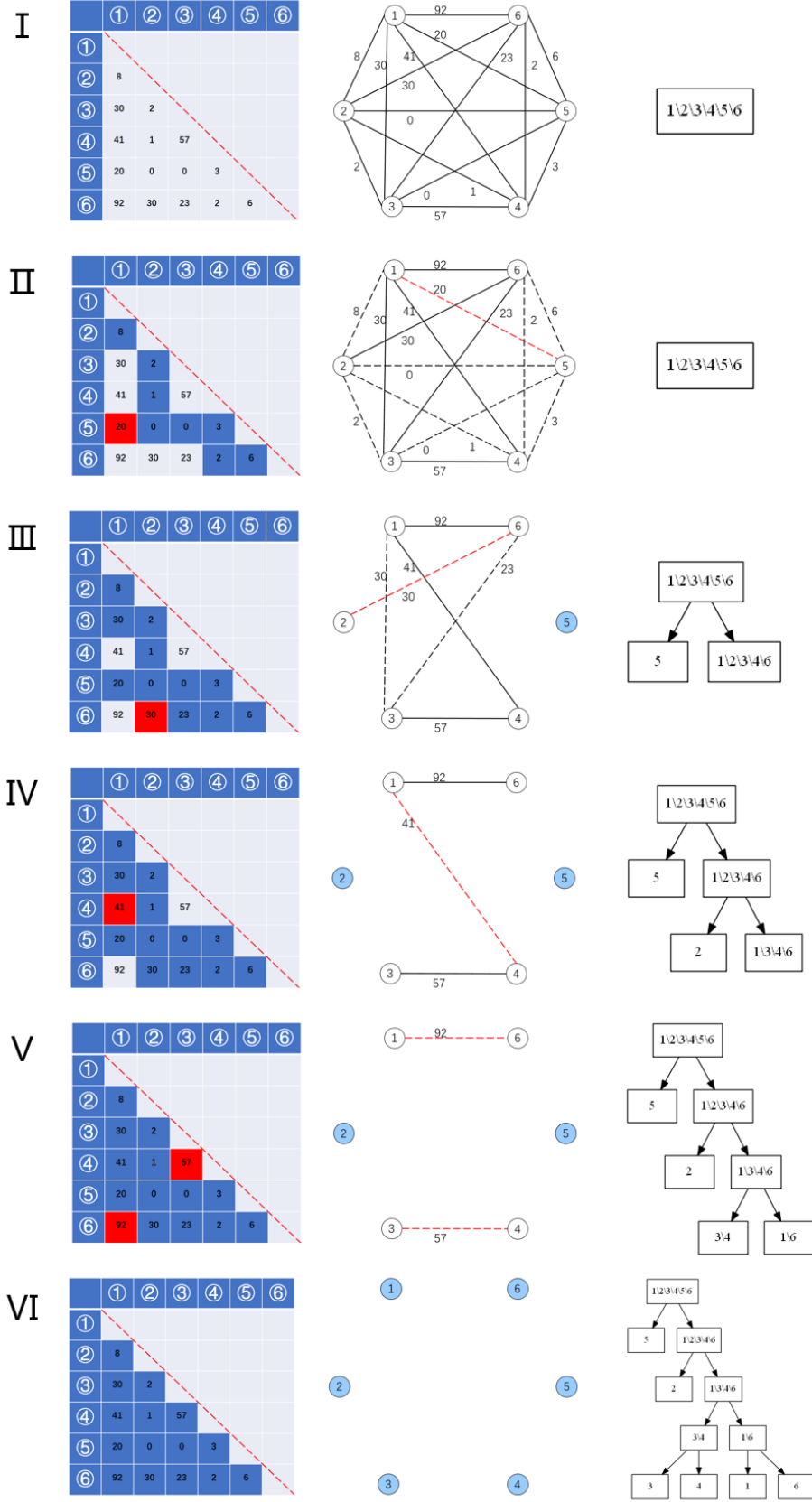


Fig 4. processing flow of minimum graph cutting algorithm

The more detailed processing flow is illustrated in Fig 4. From left to right, the sub-columns represent lower triangular matrixes, undirected graphs, and constructed dendrograms respectively. The blue cells in the left subfigures indicate that the correspondent edges have been cut off. In step II, for example, the edges with weights of 0, 1, 2, 3, 6 have been cut off and the edge with the weight of 20 will be the next one. The current cutting operation splits the graph into two subgraphs. The left child contains one node--number 5. The right child has 5 nodes which will be split in a nested fashion.

3.2.2 Tree-CNN module

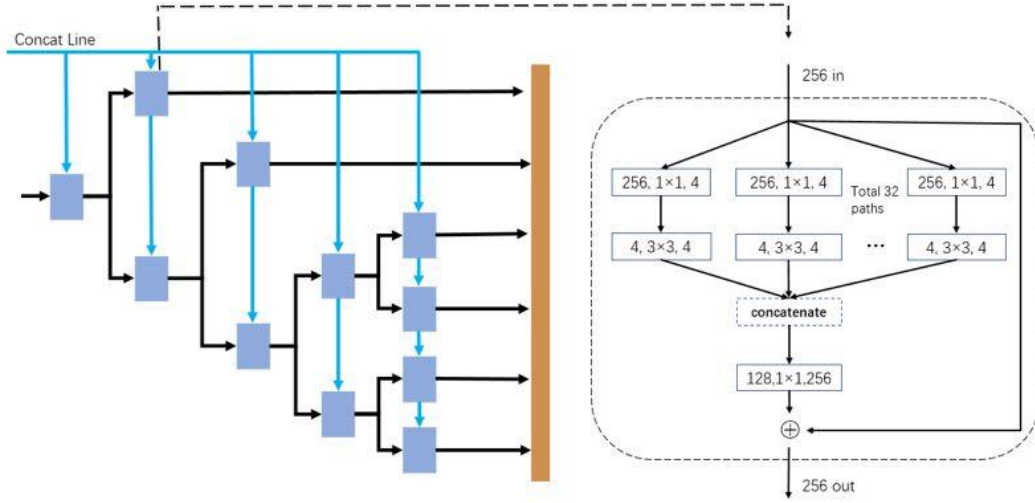


Fig 5. The Tree-CNN module

The Tree-CNN module is the core of the TreeSegNet, which can enhance the result of the previous semantic segmentation. The ISPRS dataset has six categories. Thus, in the Fig 5, the Tree-CNN module is illustrated with a binary tree which has six leaf nodes. Each node is a ResNeXt unit shown on the right-hand side in Fig 6. Through continuous optimization of back propagation, features that can easily distinct classes tend to go through the shorter path with fewer convolutional layers. In other words, the most easily confused classes tend to choose the path containing more neural layers for feature extraction. For the Tree-CNN module, it is important to use the ResNeXt units. These

units not only can avoid gradient vanishing problem causing by deeper neural layers, but also can save graphic memories by reducing the number of hyperparameters. The features entering the ResNeXt unit has two sources: the output of the previous ResNeXt unit and the concatenating features.

Concatenating connections, also called short connections, are used to transport features. The features output by the segmentation module is limited in size for the following training of Tree-CNN module. Thus, we concatenate the feature maps output by the first convolutional layer to the input channels of the ResNeXt unit just as the blue lines shown in Fig 5. This kind of connections pass the same feature map to all ResNeXt units of the Tree-CNN module, reusing the information extracted before. The number of features in the concatenating connections is relevant to the overall accuracy. In the experiment, we tested 16, 32 and 64 features to find the best feature reusing degree.

The TreeSegNet is a fully convolutional neural network. It has no fully connected layers. After the Tree-CNN module, all features are passed into a 1×1 convolutional layer and updated weights by SOFTMAX loss function before outputting.

4. Implementation details

4.1 Data preprocessing

The Potsdam dataset of the ISPRS contains 2D multi-spectral remote sensing images. They are stored in the form of RGB, IRRG and DSM. Before entering the TreeSegNet, the grouped channels of images need to be split and transformed into five channels in a single image pattern.

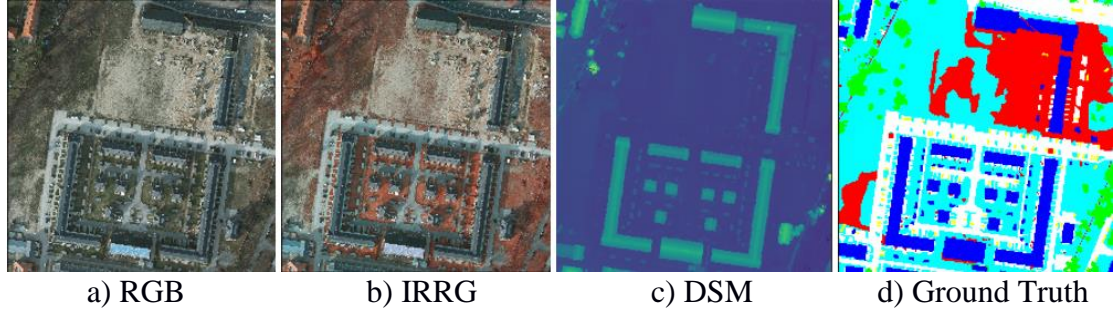


Fig 6. An example of Potsdam images.

These images are then performed data augmentation by image transformation, clipping and rotation. Since the aerial imageries are orthogonal images photographed from the topside, they are rotated by every 10 degrees repeatedly in 360 degrees to maximize the data. For each 6000x6000 VHR image, 36 images are obtained after the rotation. According to the following steps, we calculate the maximum horizontal square in the rotated images showed in Fig 7.b) and clip it out. All the three squares share the same center positions.

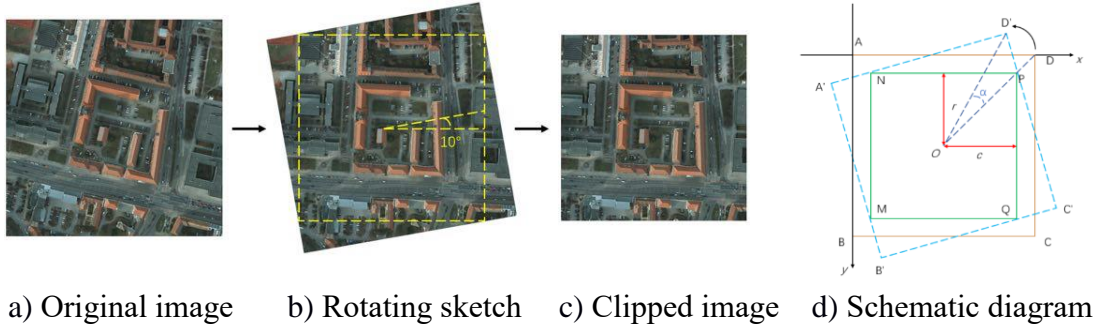


Fig 7. Image augmentation.

As shown in Fig 7.d), the coordinate of point A is $(0, 0)$. Assuming the length of the original square is $2d$, the coordinates of points B, C, D and O are $(0, 2d)$, $(2d, 2d)$, $(2d, 0)$ and (d, d) respectively. The original image is rotated by α degree counterclockwise on its center point O. According to geometry, the new position A' is calculated by the following equation.

$$\begin{cases} x_{A'} = x_O + (x_A - x_O) \cos \alpha - (y_A - y_O) \sin \alpha \\ y_{A'} = y_O + (x_A - x_O) \sin \alpha + (y_A - y_O) \cos \alpha \end{cases}$$

The vertexes of the new clipped square that are labeled by M, N, P, Q can be computed by $(d + c, d - r)$, $(d + c, d + r)$, $(d - c, d + r)$, and $(d - c, d - r)$ respectively, where

$$\begin{cases} c = -\frac{a_1 c_2 + a_2 c_1}{a_2 b_1 + a_1 b_2} \\ r = -\frac{b_1 c + c_1}{a_1} \end{cases}$$

and

$$\begin{cases} a_1 = y_{B'} - y_{A'} \\ b_1 = x_{A'} - x_{B'} \\ c_1 = x_{B'} \cdot y_{A'} - x_{A'} \cdot y_{B'} \end{cases}$$

4.2 Overlap tiles

The obtained square images are still too big for training. We have to further clip the large image into tiles, and test the tiles one by one from bottom left to up right in a sliding window way. For very high resolution images, we propose an overlap tiles strategy. Using overlapped tiles is not only because of the limitation of GPU memory but also brings more training data and thus improve the segmentation accuracy.



Fig 8. Overlap tiles

The big squares contain boundaries fields. These fields are overlapped areas. The small

squares are in fact tiled across the image. According to the strategy, only the very center pixels of big squares directly use the prediction value. For overlap areas, we compute the weight by the Gaussian function in which the parameter σ is the distance between the position of the current pixel and the center of the tile.

$$G(x, y) = \frac{1}{2\pi\sigma^2} - (x^2 + y^2)/2\sigma^2$$

Through weighted summary, we composite the overlap tiles and seamless stitch the whole segmental image. In the cases that pixels are in the border region of the image, the missing context is extrapolated by mirroring the input image.

4.3 Training

The TreeSegNet is implemented on the MXNet. The MXNet is a GPU friendly deep learning framework that provides two ways to program: shallow embedded mode and deep embedded mode. We use the deep embedded mode to realize the TreeSegNet. The network defines the convolutional layer, the ReLU layer, and the pooling layer by the SVM model of the MXNet.

To minimize the overhead and make maximum use of the GPU memory, we favor large input tiles over a large batch size. For two NVidia 1080Ti GPU, we choose 640×640 square images, hence the batch size cannot be larger than to 8. The epoch that is the number of learning steps is initially set to 80. We use a high momentum (0.9). The initial learning rate is 0.01 when the number of training steps reaches half of the total learning steps and the learning rate is adjusted to 0.001. When the number of training steps reaches 3/4 of the total learning step, set the learning rate at 0.0001.

5. Experiments and analysis

To validate the effectiveness of the TreeSegNet, experiments are carried out on the ISPRS Potsdam 2D labeling dataset. We first compare the proposed method with the state

of the art methods including the RIT_L7, FCN, FCN&CRF and etc. We also applied the DeepUNet to semantic segmentation of Potsdam 2D remote sensing images under the same experimental environments. Then detailed analyses are performed by adjusting training parameters, tuning network structures, and using different Tree-CNN structures.

5.1. Experimental environments

The experiments are carried out on a laboratory computer. Its configuration is shown in Table 1. The operating system is installed of Ubuntu 16.04. The main required packages include python 2.7, CUDA8.0, cuDNN7, Tensorflow1.1.0, Caffe, Keras1.2.0, MXNet0.10.0 and etc.

Table 1. Experimental environments

CPU	Intel (R) Core (TM) i7-4790K 4.00Hz
GPU	GeForce GTX1080 Ti
RAM	20GB
Hard disk	Toshiba SSD 512G
System	Ubuntu 16.04

5.2 Dataset

The experiments use the 2D semantic labeling contest, Potsdam dataset released by ISPRS Commission II/4[44], a remote sensing research dataset describes the environment and surroundings in and around the city. This dataset, using a digital aerial camera to take a vertical shot of multiple parts of a site, includes 38 image patches, each consists of a very high resolution true orthophoto (TOP) and its corresponding digital surface model (DSM), in which 24 images with ground truth labels are used for model training, and the other 14 images are for the testing. It includes six most common land cover classes,

including impervious surfaces (Imp_Surf), buildings (Building), low vegetation (Low_veg), trees (Tree), cars (Car) and clutter/background (Clutter). The dataset contains city and suburb of artificial surface extensive use of filling mixture formation (such as concrete, steel, and wooden roof) and semi-natural environment (such as artificial grassland, bare soil). ISPRS shows that the suburbs of the city contain a small number of trees, bushes, cars, and sundries.

In Section 5.4, when TreeSegNet compares experimental results with most state-of-the-art methods, we use all 24 labeled images for training and 14 unlabeled images for testing. In the experiments to analyze the structure and parameters of TreeSegNet, we divided the 24 labeled images into a training set (18 images) and a validation set (5 images), and remove one image (numbers 7_10) out of the experiment.

5.3 Evaluation matrix

The performance of the TreeSegNet is evaluated on ISPRS Potsdam 2D dataset with respect to overall accuracy (OA) and F1 score on each class. The OA measures the global accuracy of semantic segmentation, providing information about the rate of correctly classified pixels. The OA and F1 score can be calculated by the following formulas:

$$OA = \frac{tp + tn}{p + n}$$

$$F1 = 2 \times \frac{precision \times recall}{precision + recall}$$

$$precision = \frac{tp}{tp + fp} \quad recall = \frac{tp}{tp + fn}$$

where in the confusion matrix, the True Positive (TP) is the value of the correspondent diagonal elements. The False Positive (FP) is computed from the summation of the column, while the False Negative (FN) is the summation of the row, excluding the main diagonal element.

5.4 Results and analysis

5.4.1 Overall performance

On the ISPRS Potsdam website, we have not found public results by U-Net which obtain great success for semantic segmentation. To verify the proposed method, we re-implemented U-Net (BUCT1) and applied them to Potsdam 2D semantic labeling.

We submitted our results on the unlabeled test images to ISPRS organizers for evaluation. The result images are visually illustrated in Fig 9 and the detailed numerical metrics are listed in Table 2. The TreeSegNet (BUCTY4) ranks 1st both in mean F1 score and OA, compared with other published works. As can be seen from Table 2, the segmentation result of TreeSegNet takes the first place in each category, except for the tree class.

In the comparison with DST_5 in Building and Car categories, the TreeSegNet got 0.9% and 1.1% higher F1 scores. The performance of U-Net is also competitive. Compared with the U-Net, the TreeSegNet got 0.5%, 0.3%, 0.5%, 0.9% and 1.9% higher F1 scores in imp_surf, building, low_veg, tree and car classes.

Table 2. Quantitative comparisons between our method and other related methods (already published) on ISPRS test set.

Method	Imp_Surf	Building	Low_veg	Tree	Car	OA	Mean F1
SVL_1	83.5	91.7	72.2	63.2	62.2	77.8	74.6
DST_5[3]	92.5	96.4	86.7	88.0	94.7	90.3	91.7
UZ_1[39]	89.3	95.4	81.8	80.5	86.5	85.8	86.7
RIT_L7[40]	91.2	94.6	85.1	85.1	92.8	88.4	89.8
KLab_2[41]	89.7	92.7	83.7	84.0	92.1	86.7	88.4
GSN[29]	92.2	95.1	83.7	89.9	82.4	90.3	88.7

DeconvNet[4]	82.4	85.8	69.1	66.7	75.3	19.5	76.3
U-Net	92.4	97.0	86.3	86.4	93.9	90.0	91.2
TreeSegNet	92.9	97.3	86.8	87.3	95.8	90.5	92.0

In Fig 9, we mainly show the detailed results of the test image (top_Potsdam_2_13_class.tif). The figures are divided into two groups. The first group shows the situation of whole images. The second group magnified the local details. The first column of each group is the original test image and its segmentation results of related methods. The second column displays the evaluation images, where red pixels represent those are wrongly segmented and green ones vice visa. It can be found that the TreeSegNet produces fewer segmentation errors, especially in the tree and low_veg categories.

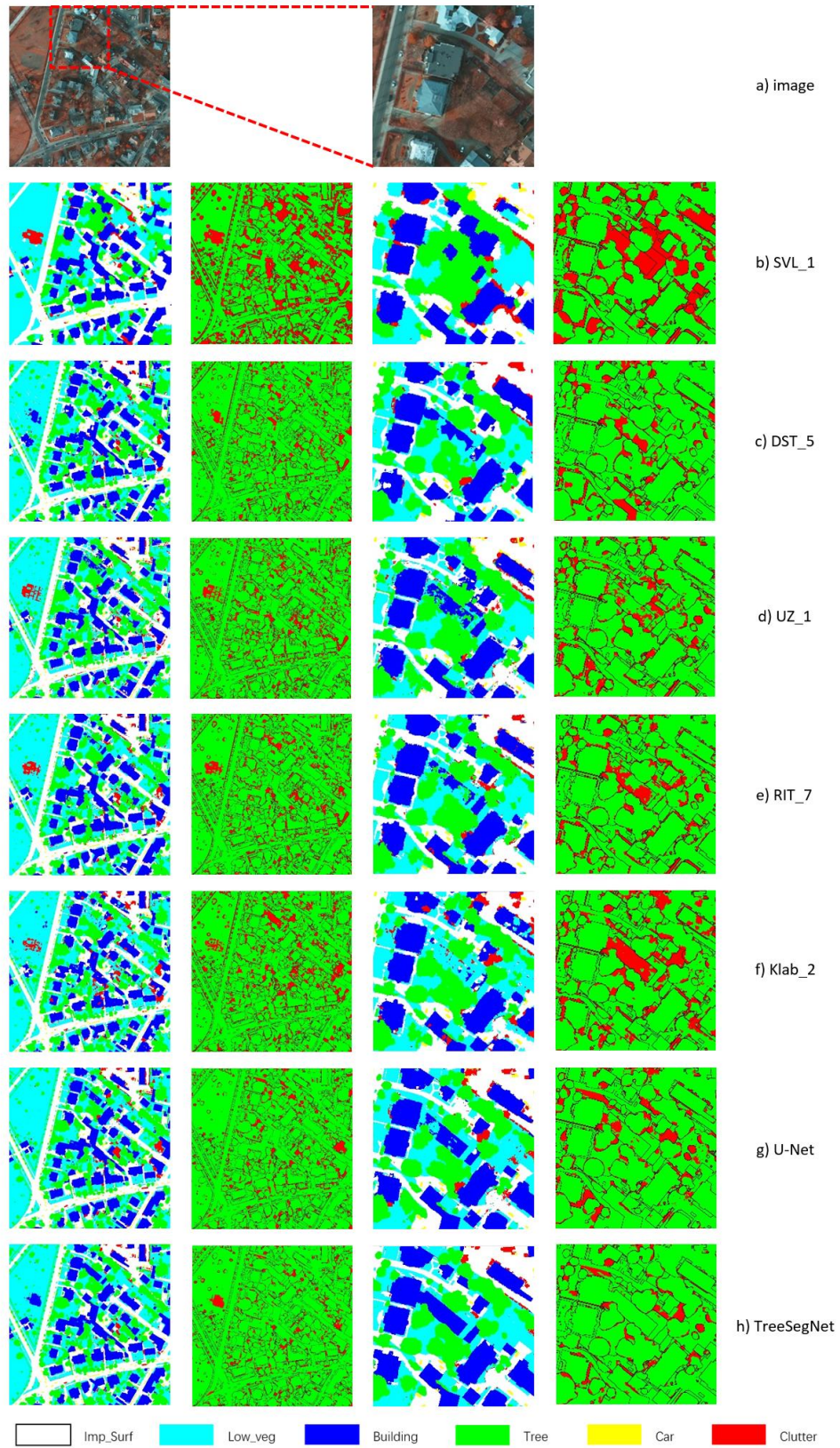


Fig 9. Global and local detailed results of “top_Potsdam_2_13_class.tif”.

Fig 10 illustrates another segmentation sample of “top_Potsdam_5_15_class.tif”. The first column is the global segmentation result, and the second and the third column are some detail magnified parts of the image. In the second column, we can find the phenomenon that the TreeSegNet clearly distinguishes tree areas from low_veg areas. In fact, without the Tree-CNN block, the areas of low_veg and imp_surf are more likely to be classified into tree and clutter respectively. In the third column, for tiny objects like cars, our results are still satisfactory by the reduction and disappearance of adhesion and bubble-effect. Moreover, among these compared methods, the TreeSegNet obtains the smoothest and most coherent boundary for the building class in segmentation results.

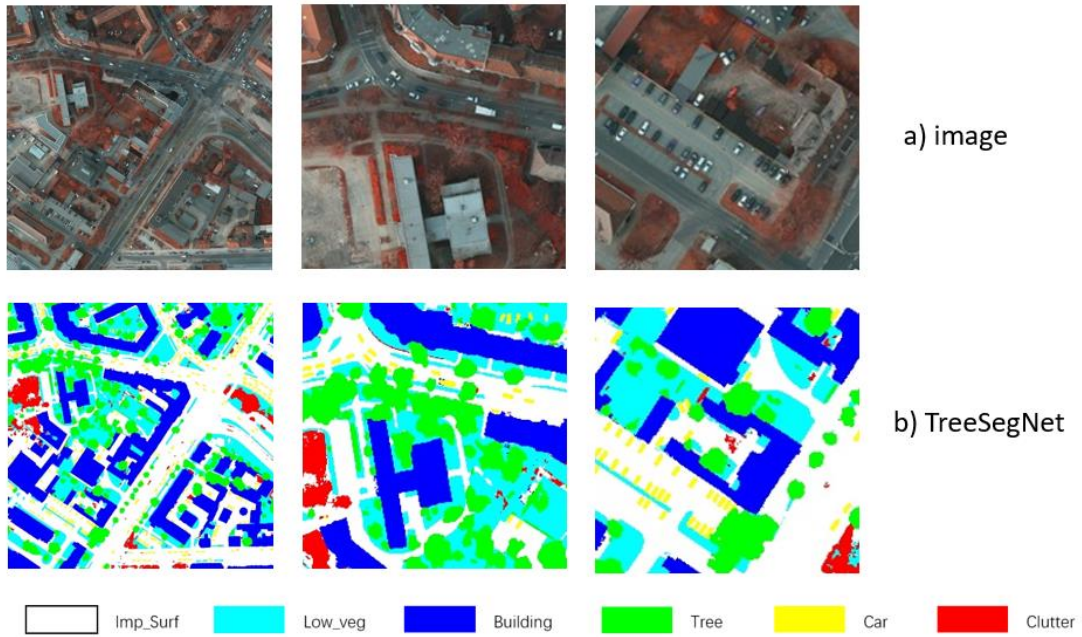


Fig 10. Segmentation results of “top_Potsdam_5_15_class.tif”.

It should be noted that the results of above-listed methods are not to be exactly compared under the same conditions. For example, KLab_2 trains the module on their own expanded dataset named RIT-18. Differently but not contradictorily, the TreeSegNet aims to establish an end-to-end network architecture for dealing with imbalanced data and easily confused categories, suitable for VHR imageries.

5.4.2 Improvement by TreeSegNet

We adopted the DeepUNet to this problem and use it as the baseline for comparisons.

Table 3 below shows the improvement brought by TreeSegNet.

Table 3. Segmentation results for DeepUNet and TreeSegNet.

Method	Imp_Surf	Building	Low_veg	Tree	Car	Clutter	OA
DeepUNet	92.8	97.4	84.5	85.5	95.1	44.7	89.4
TreeSegNet	92.9	97.3	86.8	87.3	95.8	51.1	90.5

The training of DeepUNet is the first phase of the TreeSegNet. It provided the first pass running result for the TreeSegNet. With the Tree-CNN module, the TreeSegNet is improved significantly. The OA is increasing from 89.4% to 90.5%.

In Fig 11, we show the image of “top_Potsdam_5_15_class.tif” and its segmentation results. This image contains lots of easy-confused trees and low_veg. As it is shown in Table 4, the F1 scores of low_veg and tree classes obtain 2.2% and 1.3% increasement respectively compared with the original DeepUNet.

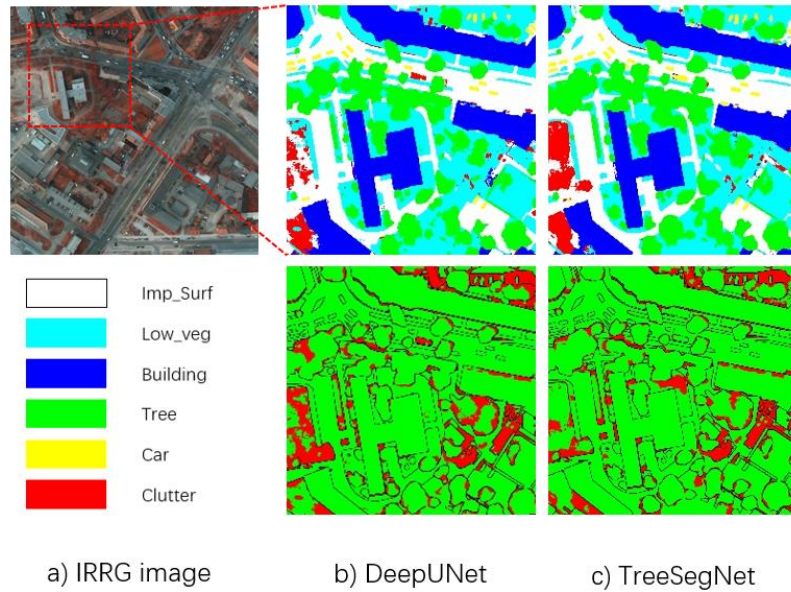
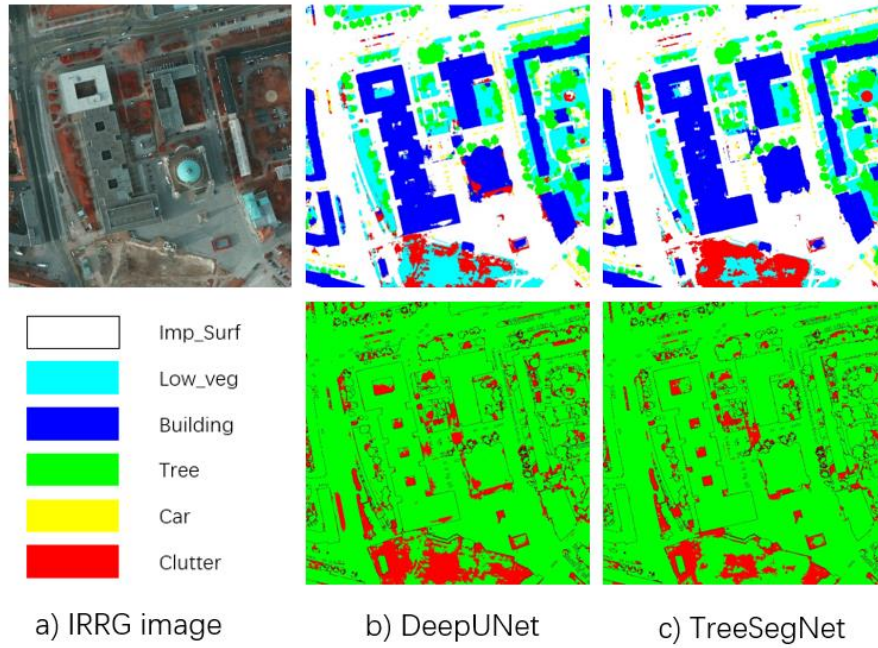


Fig 11. Local details of segmentation on “top_Potsdam_5_15_class.tif”.

Table 4. The evaluation results of “top_Potsdam_5_15_class.tif”

Method	Imp_Surf	Building	Low_veg	Tree	Car	Clutter	OA
DeepUNet	92.2	97.3	80.8	86.7	95.7	47.8	89.0
TreeSegNet	93.3	97.6	83.0	88.0	96.0	59.7	90.6

Fig 12 shows the segmentation results of “top_Potsdam_7_13_class.tif”. The corresponding accuracy of the six categories of DeepUNet and TreeSegNet are shown in Table 5. In this image, the improvement of segmentation results for the imp_surf and clutter is obvious, increasing 8% and 21.7% respectively.

**Fig 12.** Local details of segmentation on “top_Potsdam_7_13_class.tif”.**Table 5.** The evaluation results of “top_Potsdam_7_13_class.tif”

Method	Imp_Surf	Building	Low_veg	Tree	Car	Clutter	OA
DeepUNet	93.9	95.5	69.6	80.1	95.6	48.0	87.3
TreeSegNet	94.6	96.3	77.6	80.1	95.1	69.7	90.3

For the next groups of experiments in Section 5.4.3 and Section 5.4.4, we divide the labeled Potsdam datasets into two parts, 18 images as the training set, and 5 images (image numbers 7_7, 7_8, 7_9, 7_11, 7_12) as the validation set. The image numbered 7_10 has error annotations, which will bring about the degradation of the network segmentation performance. So, it is removed from experiments. Following results are reported on the validation set if not specified.

5.4.3 Different tree structures

The Tree-CNN structures have many choices, for example, using binary balanced tree structure or directly increasing convolutional layers. It is necessary to prove that the higher OA of TreeSegNet is not brought by deeper neural layers or broad network structures. Therefore, we compare different tree structures including Fig 13.(a), and Fig 13.(b) in the same condition to further understand the TreeSegNet. Actually, the training of TreeSegNet contains more than one pass. For the first pass, the DeepUNet is trained. Then the TreeSegNet is constructed from the confusion matrix. It will be retrained in the second pass. Then a new confusion tree is constructed. These steps are iterated until the Tree-CNN Block is convergent. According to the experimental results, the evolution of the confusion trees are changing from none to Fig 13.(c), and then to Fig 13.(d). Table 6 shows the comparison results. The TreeSegNet with convergent confusion tree structure showed in Fig 13.(d) got the highest OA of 90.66%. The number of features on the concatenating connection we use for this set of experiments is 64.

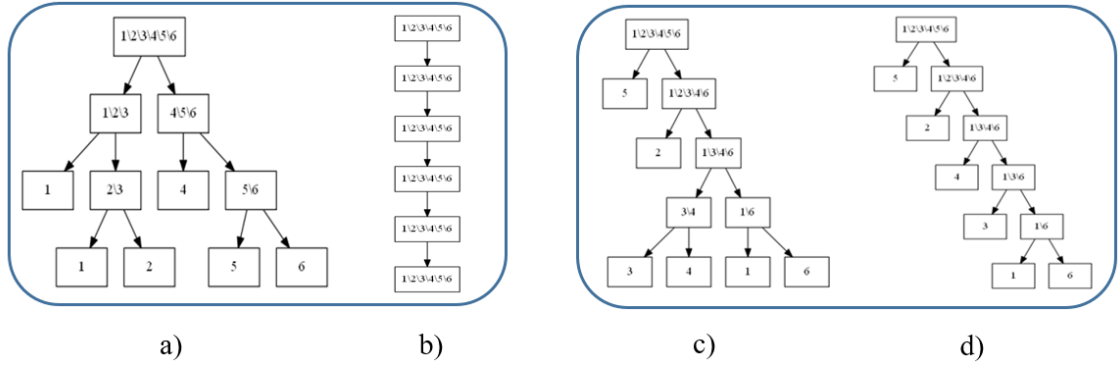


Fig 13. Different tree structures

Table 6. The evaluation OA of validation set for different structure

Structure	OA
TreeSegNet with no tree	88.43
TreeSegNet + balanced tree	89.88
TreeSegNet + straight structure	89.22
TreeSegNet + 1 pass	90.61
TreeSegNet + 2 passes	90.66

5.4.4 Different concatenating features

The number of features on the concatenating connection is a key parameter. We tried different numbers of features in the concatenating connections, using 16, 32, and 64 respectively. The OA for three different feature numbers are shown in Fig 13. According to the highest OA of 90.6%, we select 64 as the number of features in concatenating connections. The tree structure used in this set of experiments is Fig 13.(b).

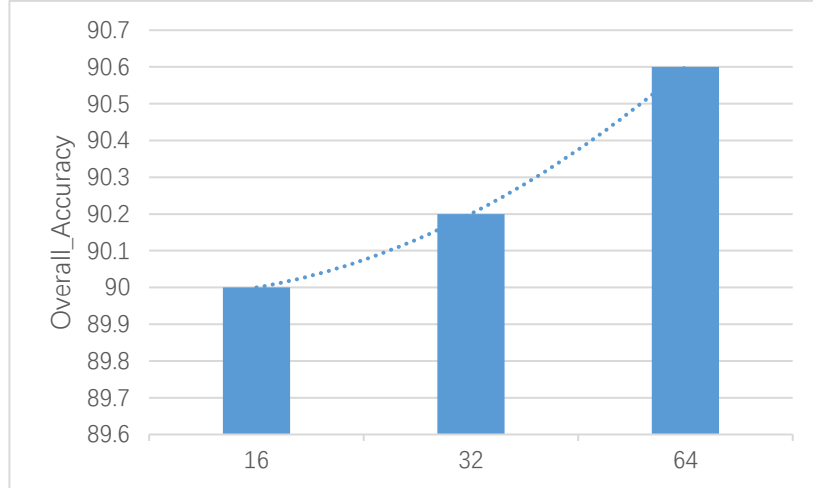


Fig 14. Influence of the number of features in the concatenating connections on the OA.

6. Conclusion

In this paper, we propose a new approach to deal with the semantic segmentation of very-high-resolution remote sensing images, using the TreeSegNet with an automatic constructed Tree-CNN module. This method performs well on the class-imbalance problem. In the experiments on ISPRS Potsdam images, the F1 measure values of the easy-confused categories are all improved. Finally, we got the highest OA among the already opened list of state-of-the-art methods.

In the future, other data augmentation methods could be considered, for example, using GAN. Since we use the original DSM for training and testing, feature fusion or normalization of DSM could also be added to the proposed method, which may further improve the accuracy.

7. Acknowledgment

The authors would like to acknowledge the provision of the datasets by ISPRS and BSF Swiss photo, released in conjunction with the ISPRS, led by ISPRS WG II/4.

References

- [1]. A. Krizhevsky, I. Sutskever, and G. E. Hinton, “Imagenet classification with deep convolutional neural networks,” in Proc. NIPS, 2012, pp. 1097–1105.
- [2]. Long J, Shelhamer E, Darrell T. Fully convolutional networks for semantic segmentation[C]//Proceedings of the IEEE Conference on Computer Vision and Pattern Recognition. 2015: 3431-3440.
- [3]. Sherrah J. Fully convolutional networks for dense semantic labelling of high-resolution aerial imagery[J]. arXiv preprint arXiv:1606.02585, 2016.
- [4]. Zeiler M D, Fergus R. Visualizing and understanding convolutional networks[C]//European conference on computer vision. Springer, Cham, 2014: 818-833.
- [5]. Badrinarayanan V, Kendall A, Cipolla R. SegNet: A deep convolutional encoder-decoder architecture for image segmentation[J]. arXiv preprint arXiv:1511.00561, 2015.
- [6]. Ronneberger O, Fischer P, Brox T. U-net: Convolutional networks for biomedical image segmentation[C]//International Conference on Medical Image Computing and Computer-Assisted Intervention. Springer, Cham, 2015: 234-241.
- [7]. Volpi M, Tuia D. Dense semantic labeling of subdecimeter resolution images with convolutional neural networks[J]. IEEE Transactions on Geoscience and Remote Sensing, 2017, 55(2): 881-893.
- [8]. Liu Y, Piramanayagam S, Monteiro S T, et al. Dense semantic labeling of very-high-resolution aerial imagery and LiDAR with fullyconvolutional neural networks and higher-order crfs[C]//Proceedings of the IEEE Conference on Computer Vision and Pattern Recognition (CVPR) Workshops, Honolulu, USA. 2017.
- [9]. Kemker R, Kanan C. Deep neural networks for semantic segmentation of multispectral remote sensing imagery[J]. arXiv preprint arXiv:1703.06452, 2017.

- [10]. Li R, Liu W, Yang L, et al. DeepUNet: A Deep Fully Convolutional Network for Pixel-level Sea-Land Segmentation[J]. arXiv preprint arXiv:1709.00201, 2017.
- [11]. Shi J, Malik J. Normalized cuts and image segmentation[J]. IEEE Transactions on pattern analysis and machine intelligence, 2000, 22(8): 888-905.
- [12]. Boykov Y Y, Jolly M P. Interactive graph cuts for optimal boundary & region segmentation of objects in ND images[C]//Computer Vision, 2001. ICCV 2001. Proceedings. Eighth IEEE International Conference on. IEEE, 2001, 1: 105-112.
- [13]. Grady L. Random walks for image segmentation[J]. IEEE transactions on pattern analysis and machine intelligence, 2006, 28(11): 1768-1783.
- [14]. Grady L, Schwartz E. Isoperimetric graph partitioning for data clustering and image segmentation[R]. Boston University Center for Adaptive Systems and Department of Cognitive and Neural Systems, 2003.
- [15]. Di Y, Jiang G, Yan L, et al. Multi-Scale Segmentation of High Resolution Remote Sensing Images by Integrating Multiple Features[J]. The International Archives of Photogrammetry, Remote Sensing and Spatial Information Sciences, 2017, 42: 247.
- [16]. Ye wei, Wang Yuanjun, 2009. Minimum Spanning Tree Image Segmentation Method Based on Mumford-Shah Model[J]. Journal of Computer-Aided Design & Computer Graphics, 21(8):1127-1134.
- [17]. Cui W, Zhang Y. An effective graph-based hierarchy image segmentation[J]. Intelligent Automation & Soft Computing, 2011, 17(7): 969-981.
- [18]. S. Reis and K. Tasdemir, "Identification of hazelnut fields using spectral and Gabor textural features," ISPRS J. Photogramm. Remote Sens., vol. 66, no. 5, pp. 652–661, Sep. 2011.
- [19] Y. O. Ouma, J. Tetuko, and R. Tateishi, "Analysis of co-occurrence and discrete

wavelet transform textures for differentiation of forest and non-forest vegetation in very-high-resolution optical-sensor imagery,” *Int. J. Remote Sens.*, vol. 29, no. 12, pp. 3417–3456, May 2008.

[20] T. Wang, H. Zhang, H. Lin, and C. Fang, “Textural–spectral feature-based species classification of mangroves in Mai Po Nature Reserve from Worldview-3 imagery,” *Remote Sens.*, vol. 8, no. 1, pp. 24-1–24-15, Dec. 2015.

[21] H. Yu, W. Yang, G.-S. Xia, and G. Liu, “A color-texture-structure descriptor for high-resolution satellite image classification,” *Remote Sens.*, vol. 8, no. 3, pp. 259-1–259-24, Mar. 2016.

[22] S. Li, S. Wang, Z. Zheng, D. Wan, and J. Feng, “A new algorithm for water information extraction from high resolution remote sensing imagery,” in *Proc. IEEE Int. Conf. Image Process. (ICIP)*, Sep. 2016, pp. 4359–4363.

[23]. Yu F, Koltun V. Multi-scale context aggregation by dilated convolutions[J]. arXiv preprint arXiv:1511.07122, 2015.

[24]. Chen L C, Papandreou G, Schroff F, et al. Rethinking atrous convolution for semantic image segmentation[J]. arXiv preprint arXiv:1706.05587, 2017.

[25]. Chen L C, Papandreou G, Kokkinos I, et al. Deeplab: Semantic image segmentation with deep convolutional nets, atrous convolution, and fully connected crfs[J]. *IEEE transactions on pattern analysis and machine intelligence*, 2018, 40(4): 834-848.

[26]. Badrinarayanan V, Kendall A, Cipolla R. SegNet: A deep convolutional encoder-decoder architecture for image segmentation[J]. arXiv preprint arXiv:1511.00561, 2015.

[27]. Lin G, Milan A, Shen C, et al. Refinenet: Multi-path refinement networks for high-resolution semantic segmentation[C]//*IEEE Conference on Computer Vision and*

Pattern Recognition (CVPR). 2017.

[28] Ronneberger O, Fischer P, Brox T. U-net: Convolutional networks for biomedical image segmentation[C]//International Conference on Medical image computing and computer-assisted intervention. Springer, Cham, 2015: 234-241.

[29]. Wang H, Wang Y, Zhang Q, et al. Gated convolutional neural network for semantic segmentation in high-resolution images[J]. Remote Sensing, 2017, 9(5): 446.

[30]. Niculescu-Mizil A, Caruana R. Predicting good probabilities with supervised learning[C]//Proceedings of the 22nd international conference on Machine learning. ACM, 2005: 625-632.

[31]. Zadrozny B, Elkan C. Transforming classifier scores into accurate multiclass probability estimates[C]//Proceedings of the eighth ACM SIGKDD international conference on Knowledge discovery and data mining. ACM, 2002: 694-699.

[32]. López V, Fernández A, García S, et al. An insight into classification with imbalanced data: Empirical results and current trends on using data intrinsic characteristics[J]. Information Sciences, 2013, 250: 113-141.

[33]. Team R C. R: A language and environment for statistical computing [Internet]. Vienna, Austria: R Foundation for Statistical Computing; 2014[J]. 2015.

[34]. Olvera-López J A, Carrasco-Ochoa J A, Martínez-Trinidad J F, et al. A review of instance selection methods[J]. Artificial Intelligence Review, 2010, 34(2): 133-143.

[35]. Liu H, Yu L. Toward integrating feature selection algorithms for classification and clustering[J]. IEEE Transactions on knowledge and data engineering, 2005, 17(4): 491-502.

[36]. Breiman L. Bagging predictors[J]. Machine learning, 1996, 24(2): 123-140.

[37]. Freund Y, Schapire R E. A decision-theoretic generalization of on-line learning and

an application to boosting[J]. Journal of computer and system sciences, 1997, 55(1): 119-139.

[38]. Benites F, Sapozhnikova E. Learning different concept hierarchies and the relations between them from classified data[J]. Intel. Data Analysis for Real-Life Applications: Theory and Practice, 2012: 18-34.

[39]. Bischke B, Helber P, Folz J, et al. Multi-Task Learning for Segmentation of Building Footprints with Deep Neural Networks[J]. 2017.

[40]. Iglovikov V, Shvets A. TerausNet: U-Net with VGG11 Encoder Pre-Trained on ImageNet for Image Segmentation[J]. 2018.

[41]. Yang S, Chen L F, Yan T, et al. An ensemble classification algorithm for convolutional neural network based on AdaBoost[C]//Computer and Information Science (ICIS), 2017 IEEE/ACIS 16th International Conference on. IEEE, 2017: 401-406.

[42]. Frosst N, Hinton G. Distilling a Neural Network Into a Soft Decision Tree[J]. arXiv preprint arXiv:1711.09784, 2017.

[43]. Simonyan K, Zisserman A. Very deep convolutional networks for large-scale image recognition[J]. arXiv preprint arXiv:1409.1556, 2014.

[44]. ISPRS 2D semantic labeling contest - Potsdam.

<http://www2.isprs.org/commissions/comm3/wg4/2d-sem-label-potsdam.html>. Accessed April 15, 2018